34th EPS Conference on Plasma Phys. Warsaw, 2 - 6 July 2007 ECA Vol.**31F**, O-4.006 (2007)

Laser Interactions with Low-Density Foams for Laser Beam Smoothing and X-ray Source Studies

J. Limpouch[1], O. Renner[2], E. Krousky[2], W. Nazarov[3], N.G. Borisenko[4], N.N. Demchenko[4], S.Yu. Gus'kov[4], D. Klir[1], V. Kmetik[5], R. Liska[1], K. Masek[2], Yu.A. Merkul'ev[4], M. Pfeifer[2], M. Sinor[1], J. Ullschmied[5]

[1] *Czech Technical Univ. in Prague, FNSPE, Brehova 7, 115 19 Prague, Czech Republic*
[2] *Institute of Physics, AS CR, Na Slovance 2, 182 21 Prague 8, Czech Republic*
[3] *University of St. Andrews, School of Chemistry, St. Andrews, Fife KY16 9ST, UK*
[4] *P.N. Lebedev Physical Institute of RAS, Leninskyi Ave. 53, 117 924 Moscow, Russia*
[5] *Institute of Plasma Physics, AS CR, Za Slovankou 3, 182 21 Prague 8, Czech Republic*

1. Introduction

Low-density foam layers may significantly improve the target design for various applications. Foam layers may be used in inertial fusion targets to improve implosion symmetry [1]. Alternatively, transparent underdense foam may be applied as a dynamic phase plate in order to randomize and partly wash out inhomogeneity patterns inside laser beams [2]. Foams may be also exploited for generation of quasi-homogeneous plasma for atomic physics and X-ray spectroscopy studies [3] and in astrophysics dedicated experiments [4].

In the first part of this paper, measurements of laser transmission through underdense (i.e. electron density n_{eh} in fully ionized homogenized foam is less than laser critical density n_c) foam layers of variable thicknesses are presented. Aerogel 3D networks of cellulose triacetate (TAC – $C_{12}H_{16}O_8$) with typical pore size in range 0.5-3 μm [5] were used. The laser-foam interaction physics is studied, and the laser energy losses are tested for foam application as a dynamic random phase plate for laser beam smoothing.

In the second part, very preliminary results are presented of our recent experiment studying X-ray emission in the vicinity of chlorine He-α and Ly-α lines from chlorine-doped TMPTA ($C_{15}H_{20}O_6$) aerogel foams [6]. These foams with submicron pore size are homogenized very quickly and a relatively thick, nearly homogeneous hot plasma layer is formed that may used for atomic physics studies and as a well-characterized source of line X-ray emission.

2. Laser transmission through foam layers

Third harmonics (λ = 439 nm) of PALS iodine laser was incident normally on the foam surface placed 500 μm behind the best focus, and thus, the laser spot diameter on target was 300 μm and laser irradiances were in the range of $I \approx 10^{14} - 10^{15}$ W/cm^2. The targets 100, 200 and 400 μm-thick were made of TAC of densities 2.25, 4.5 and 9 mg/cm^3. Optical streak camera was used together with a calorimeter for measurement of laser transmission through the foam targets. Measurements with foams were related to the transmission of laser pulse through the detection channel when there is no foam in the washer, i.e. laser is transmitted through a hole of the inner washer diameter ~2.5 mm.

Temporal shapes of laser pulses transmitted through foams are presented in Fig.1. In all shots, the laser pulse leading edge penetrated through transparent foam up to intensity 3×10^{12} W/cm^2, which was ≈ 0.5 - 1% of the maximum. At this intensity level, overdense plasma was formed at the pore walls and laser was reflected, scattered and absorbed in the foam. For 100 μm-thick foam layer of density 4.5 mg/cm^3 ($n_{eh} \approx 0.25\, n_c$), partial laser transparency was restored at approximately 250 ps after laser pulse maximum. The penetration is restored earlier for lower density foams when foam area mass (density multiplied by thickness) is constant (frame b). The speed of laser penetration grows slowly with laser intensity. Penetration of the laser pulse leading edge may be a disadvantage for ablation pressure smoothing, as the imprint is formed at the laser pulse rising edge.

The maximum laser transmission was approximately 60% for 100 μm-thick layer of foam density 2.25 mg/cm^3. Relatively high energy losses are here due to short (≈ 350 ps FWHM) laser pulses, losses may be acceptable for typical laser pulses of a few ns duration.

3. X-ray emission spectra from chlorine-doped foams

The emitted X-ray spectra provide an important diagnostic tool to infer local plasma

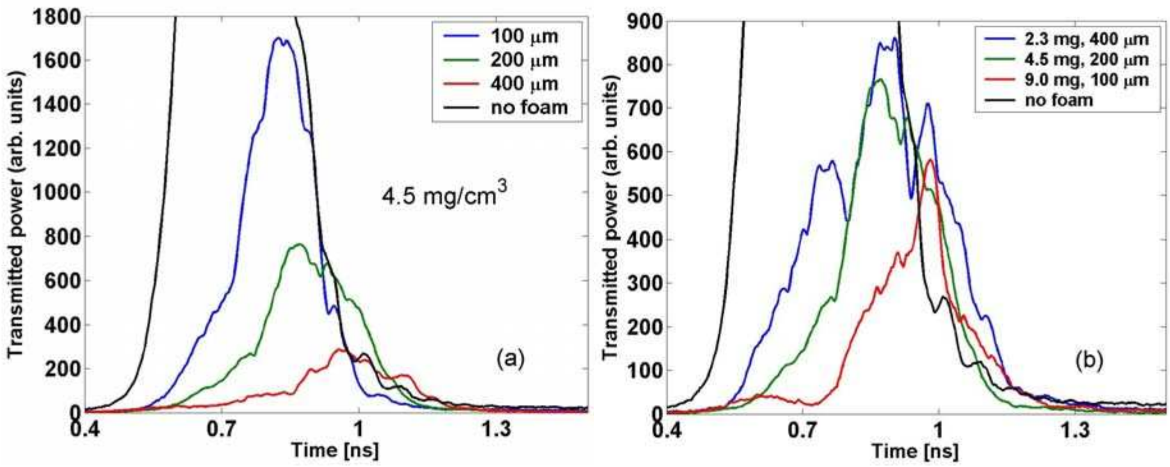

Figure 1: Laser transmission through foam layer compared to vacuum transmission. (a) Three thicknesses of the foam layer for density 4.5 mg/cm^3. (b) Constant foam area density for three different foam densities. Laser pulse of energy in range 150 – 170 J, wavelength 432 nm and duration 320 ps is incident normally on TAC.

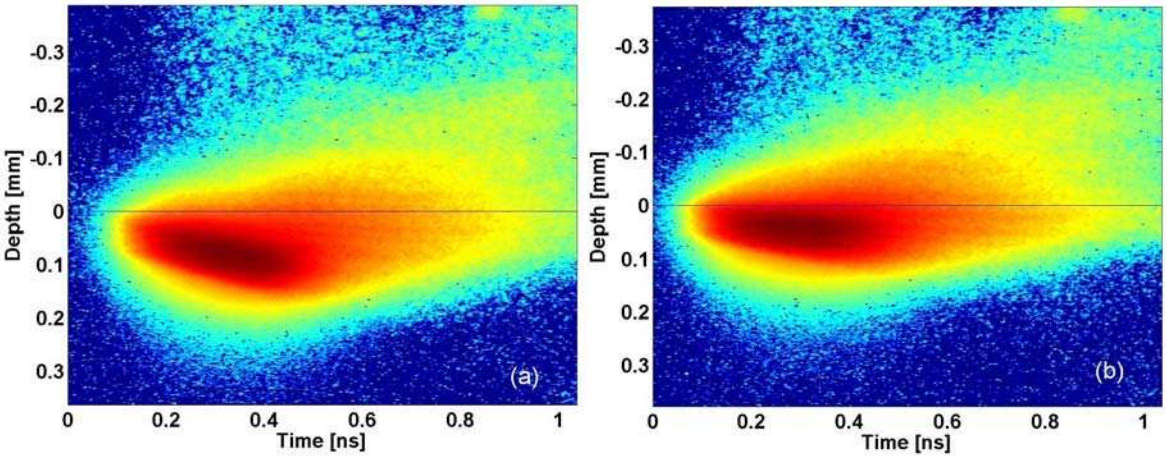

Figure 2: Side-on slit images of foam emission recorded by X-ray streak (logarithm of signal, photons above 1 keV). Laser pulse (350 ps FWHM, λ=439 nm) is incident from the top on foam surface (Depth=0), where laser spot ∅=0.3 mm (laser best focus 0.5 mm above surface). (a) foam 10 mg/cm^3, 20 weight % of Cl, E_L=157 J; (b) foam 20 mg/cm^3, 10 % of Cl, E_L=161 J.

parameters particularly ionization stage, density, and temperature. The principle diagnostics used in this experiment was a vertical-geometry Johann spectrometer (VJS). The VJS disperses the radiation in a direction parallel to the axis of the cylindrically bent crystal, i.e., as a function of the vertical divergence angle φ. The instrument provides two identical sets of spectra symmetrically disposed about the central wavelength λ_0 [7]. The VJS was fitted with a crystal of quartz (100) bent to a radius of 77.2 mm and the spectral resolution in the vicinity of chlorine He-α or Ly-α lines was > 5000. The VJS observed the spectrum emitted in direction parallel to the target surface, with spatial resolution of 8 μm normal to it. A hole widening with angle of 45° was cut through the foam washer to provide view below the foam surface. Alternatively, the hole in washer could be pointed to X-ray streak camera and the spectra below the foam surface are blocked out by the washer which is used for the detection of the foam surface with accuracy better than ±16 μm.

The X-ray streak images in Fig.2 demonstrate faster deepening of the heated layer for the foam of density 10 mg/cm^3 (n_{eh}≈0.6 n_c) than for the twice denser foam. The emitting

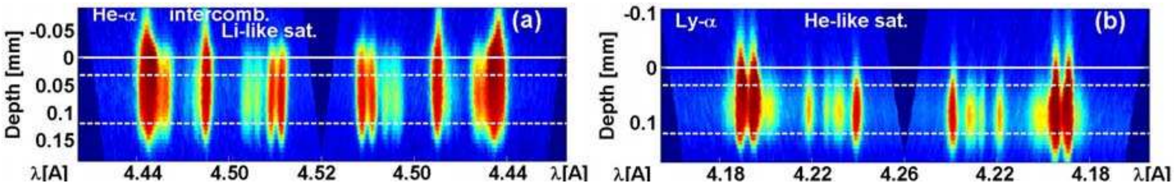

Figure 3: The processed X-ray spectra of VJS spectrograph. The line spectra are emitted by chlorine dopant (20 weight %) in TMPTA foam of density 10 mg/cm^3. Laser pulse (350 ps FWHM, λ=439 nm) is incident from the top on foam surface (Depth=0), where laser spot ∅=0.3 mm (laser best focus 0.5 mm above surface). (a) spectrum in vicinity of chlorine He-α line, E_L=128 J; (b) spectrum in vicinity of Ly-α line, E_L=151 J.

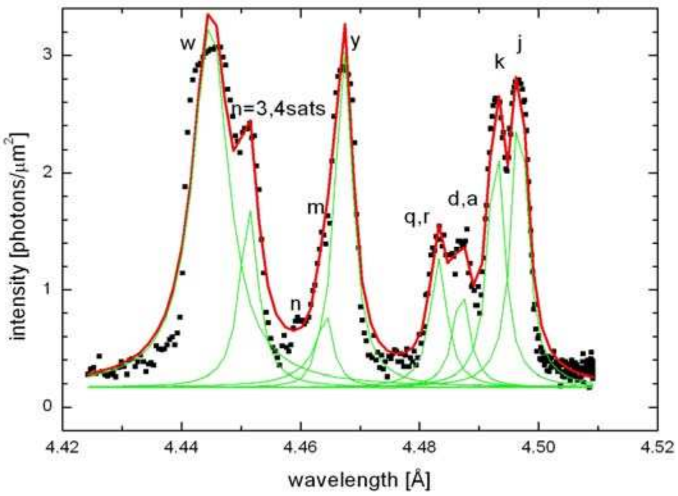

Figure 4: Decomposition of the emission spectra in vicinity of He-α line (Fig. 3a) in depth of 32 μm below the foam surface (w is the resonance He-α line, y is the intercombination line, n, m, q, r, d, a, k, j are Li-like satellites from 1s2l2l' levels, while n=3,4 denote Li-like satellites from 1s2l3l' and 1s2l4l' levels.

zone does not reach the foam layer rear side at 480 μm in any case.

The X-ray spectra, recorded by VJS in the neighborhood of chlorine He-α and Ly-α lines, are presented in Fig.3. The foam surface is marked by the full white line while the dashed lines denote the borders of the spatially uniform emission region. The cut at the depth 32 μm (position of the upper dashed line) of the left part of the spectra in Fig.3a is plotted in Fig.4 and it is decomposed to the individual spectral lines. Based on the spectra fitting of the intercombination line (y) and satellites jkl, ad, and qr (the use of mn would be too speculative) and using the FLY code, the derived plasma parameters at the distance of 32 μm below the foam surface are n_e=3±1×10^{21} cm^{-3} and T_e=410±20 eV. The plasma diameter (relevant for opacity or escape factor correction) was estimated to be 250 μm. Thus, the parameters of the heated foam plasma were deduced from line emission spectra. More detailed analysis of the experiment results is being prepared for publication, including an analysis using both spectral ranges at similar experimental parameters, the impact of foam density and of the chlorine content, and the experiment comparison with numerical simulations of the laser-foam interaction.

Acknowledgements

Support by the Czech Science Foundation Project 202/06/0801 is gratefully acknowledged.

References

[1] Dunne M., Borghesi M., Iwase A. *et al.*, *Phys. Rev. Lett.* **75**, 3858 (1995).

[2] Derkach V.N., Bondarenko S.V. *et al.*, *Laser & Particle Beams* **17**, 603 (1999).

[3] Gavrilov V.V., Gol'tsov A.Y.. *et al.*, Quantum Electronics **31**, 1071 (2001).

[4] Drake R.P., Glendinning S.G., Estabrook K. *et al.*, Phys. Rev. Lett. **81**, 2068 (1998).

[5] Borisenko N.G., Akimova I.V. *et al.*, *Fusion Sci. & Technology* **49**, 676 (2006).

[6] Nazarov W., *Fusion Sci. & Technology* **41**, 193 (2002).

[7] Renner O., Missalla T., Sondhauss P. *et al.*, *Rev. Sci. Instrum*. **68**, 2393 (1997).